

## Satellite observations of an annual cycle in the Agulhas Current

M. Krug<sup>1,2,3</sup> and J. Tournadre<sup>4</sup>

Received 9 May 2012; revised 25 June 2012; accepted 26 June 2012; published 9 August 2012.

[1] Ocean models show an annual cycle in the Agulhas Current transport which has not yet been confirmed in analyses of in-situ or satellite observations. A cross-stream coordinate approach is used to study the variability of the Agulhas Current from 18 years of along-track altimetry and merged altimetry and close to 7 years of high frequency Sea Surface Temperature (SST) observations. While the position and width of the Agulhas Current's dynamical core do not display an annual cycle, the geostrophic current speed at the current's core exhibits distinct seasonal variations, with a stronger flow observed in austral summer. The annual cycle dominates the frequency spectra of the current's core geostrophic velocities. **Citation:** Krug, M., and J. Tournadre (2012), Satellite observations of an annual cycle in the Agulhas Current, *Geophys. Res. Lett.*, 39, L15607, doi:10.1029/2012GL052335.

### 1. Introduction

[2] The Agulhas Current (AC) is the most intense western boundary current of the southern hemisphere and a key component of the global climate [Beal *et al.*, 2011]. Despite its importance at both global and regional scales, little remains known of the AC's variability with an ongoing debate on its seasonality. Numerical ocean models show annual variations in the AC transport, with a minimum in austral winter (August) and a maximum in austral summer (February) [Lutjeharms, 2006]. Previous observational studies however were unable to highlight evidence of a seasonal cycle in the AC [Matano *et al.*, 2008; Gründlingh, 1983; Bryden *et al.*, 2005]. Past analyses of observations in the AC have relied on Eulerian time-averages of moored observations or remote sensing variables to estimate the current's variability. Numerous studies have shown that stream-coordinates are better suited to estimating the true synoptic structure of western boundary currents as they minimize the contamination caused by meandering flows on the time-averaged structure of the current [Meinen and Watts, 2000]. In the case of the AC, where variations in the current's path are dominated by the intermittent passage of offshore meanders [Rouault and Penven, 2011], the choice of a stream-coordinate reference appears particularly relevant. In this paper, close to 20 years of Sea Surface

Height (SSH) observations from altimeters and 7 years of high frequency Sea Surface Temperature (SST) imagery are used to characterize the variability of the AC along the Topex / Jason altimeter's Track #020, offshore Port Elizabeth (Figure 1). Our analysis based on a stream-coordinate characterization of the AC allows us to better capture the intrinsic variability of the AC at the annual time-scale.

### 2. Method and Data

[3] Hydrographic measurements have revealed the barotropic nature of the AC [Bryden *et al.*, 2005]. Vertical profiles across the AC showed that the current had a V-shape structure with the level of no-motion reaching the sea-bed near the location of Track #020 [Casal *et al.*, 2009]. In a barotropic current, changes in SSH across the current's width can be directly related to total transport [Kelly *et al.*, 1999]. A recent study on the AC based on numerical model outputs and merged altimetry observations showed that SSH provided a good proxy for estimating variations in the current transport [van Sebille *et al.*, 2010]. In this paper, changes in the path, width and velocity of the AC's dynamical core along Track #020 (Figure 1) are used to study the variability of the AC from 1992 to 2011. Track #020 is almost perpendicular to the AC, implying that the across-track geostrophic current velocities should closely approximate the geostrophic current speeds. The properties of the AC core are established using 3 different methods applied to 1) along-track altimetry, 2) merged-altimetry maps of absolute geostrophic currents and 3) high frequency SST imagery.

[4] Method and Dataset 1): The along-track altimetry dataset is sourced from the AVISO Geophysical Data Records (GDR). The 1 Hz (5.8 km) for Topex and Jason-1 and -2 SSH data corresponding to Track #020 are collated to create an 18-year long time series. The SSH from the different missions are then inter-calibrated using the tandem missions data to provide an homogeneous data set. The overall mean SSH for Track #020 is computed and subtracted from the SSH to provide Sea Level Anomalies (SLA). This SLA record is added to the Mean Dynamic Topography (MDT) of Rio *et al.* [2011] to obtain an Absolute Dynamic Topography (ADT). The ADT are filtered using a Lee filter. This filter, based on local statistics, is known to preserve gradients well [Lee, 1981]. The across-track absolute geostrophic velocity is calculated from the filtered ADT and it is itself filtered using a Lee filter. For each cycle, a Gaussian function is fitted to the local southward current maxima detected in the along-track geostrophic velocity. The center of the AC core is defined as the location of the Gaussian peak and the shoreward and seaward edges of the AC core are taken as the distance located within  $\pm 1$  Gaussian fit standard deviation, i.e., the region where current speeds exceed half the maximum

<sup>1</sup>Ecosystem Earth Observation, Council for Scientific and Industrial Research, Cape Town, South Africa.

<sup>2</sup>Oceanography Department, Mare Institute, University of Cape Town, Cape Town, South Africa.

<sup>3</sup>Nansen-Tutu Center for Marine Environmental Research, University of Cape Town, Cape Town, South Africa.

<sup>4</sup>Laboratoire d'Océanographie Spatiale, IFREMER, Plouzané, France.

Corresponding author: M. Krug, Ecosystem Earth Observation, Council for Scientific and Industrial Research, 15 Lower Hope St., Cape Town 7700, South Africa. (mrouault@csir.co.za)

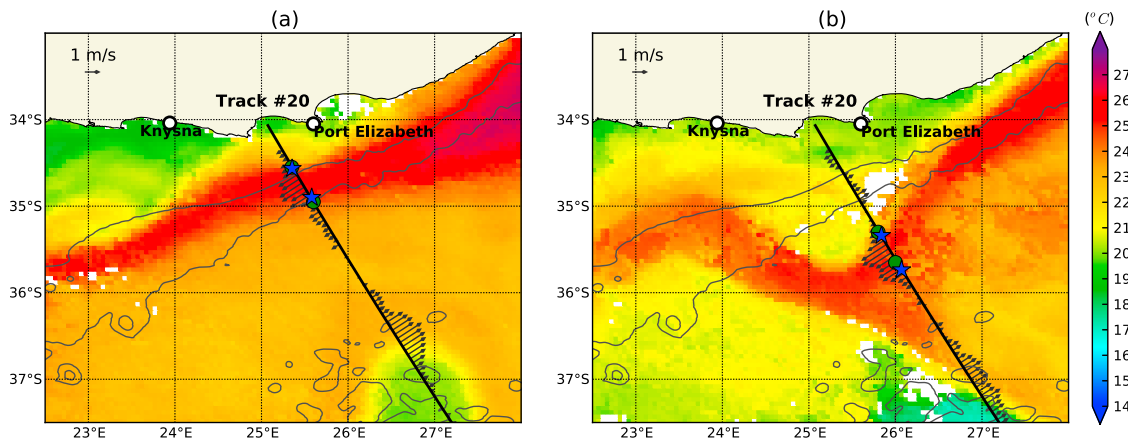


**Figure 1.** SST maps obtained (a) from 5-day weighted averages centred on the 29th of March 2010 and (b) during the passage of a large offshore meander on the 18th of May 2010. Arrows show the geostrophic currents along Topex-Jason Track #020. The AC flow is associated with a local SST maximum and strong south-westerly currents. North-easterly geostrophic currents observed east of 26°E mark the position the Agulhas Return Current. Blue stars show the edges of the AC's dynamical core estimated by fitting a Gaussian function to the local speed maximum. Green circles show the edges of the AC's dynamical core derived from the SST imagery. The 1000 m and 3000 m isobaths have been plotted as thin black contour lines.

speed. Method and Dataset 2): The position of the AC core is determined using merged maps of absolute geostrophic current (AVISO daily DT-MADT product). The AVISO product combines SLA signals from the OSTM/Jason-2, Jason-1 and Envisat altimeters to the MDT of *Rio et al.* [2011]. The AVISO product is provided on a rectilinear grid with a spatial resolution of  $1/3^\circ$  and consists in 7-day moving averages of merged SSH observations. To establish the central position of the AC core from the AVISO product, geostrophic current velocities are linearly interpolated along Track #020 at a  $0.1^\circ$  spatial resolution. The geostrophic velocities are then rotated into along-shore and across-shore components, with the along-shore component corresponding to the mean direction of the AC. The local maximum associated with the strongest along-shore flow is selected as the point where the center of the AC core lies. Method and Dataset 3): For the SST analysis, the hourly SEVIRI SST product processed by the French ERS Processing and Archiving Facility (CERSAT) and available on a  $0.05^\circ$  grid (<http://www.osi-saf.org>) is used. 5-day exponentially weighted average maps are computed from the hourly SST data. The 5-day SST averages are then extracted in a bandwidth of 15 km along Track #020 prior to running the current detection algorithm. To estimate the position and width of the AC core from the SST dataset, a method similar to that described in *Rouault and Penven* [2011] is used. The central position of the AC core is defined as the local SST maxima. The edges of the AC core are established by looking for local minima around the central position of the AC core. Figure 1 provides examples of the AC core edges detected from the along-track altimetry and the SST imagery. Variations in the position of the AC core obtained from the AVISO gridded dataset are compared to those estimated from the along-track altimetry and SST imagery. Spectral and wavelet analyses are conducted using the along-track 1 Hz altimetry data. Here, the amplitudes of the Gaussian fit to the 10-day along-track absolute geostrophic current speeds are used to identify the predominant patterns of variability for the AC core. The significance of the wavelet

and power spectrum analyses are tested using red-noise Fourier power spectrum calculated according to the method of *Gilman et al.* [1963].

### 3. Position and Width of the Agulhas Current's Dynamical Core

[5] The AC as portrayed in the 1 Hz along-track altimetry is a strong and narrow flow which exhibits rapid changes in width, speed and position (Figure 2a). Absolute geostrophic current speeds within the AC vary around a mean of  $1.4 \text{ m s}^{-1}$  and occasionally exceed  $2 \text{ m s}^{-1}$ , with the maximum value reaching  $2.8 \text{ m s}^{-1}$ . At the AC core, the standard deviation of the along-track current velocity is equal to  $0.3 \text{ m s}^{-1}$ . Previous measurements [*Lutjeharms, 2006*] have shown that current velocities across the AC increase nearly linearly from the coast to the location of the current maxima, followed by a more progressive decrease in current speeds offshore. The anisotropic nature of the AC's cross-stream velocity is also observed in the along-track altimetry (Figure 1). The Gaussian fit method used on the along-track altimetry can be considered as a first order approximation of the AC core that captures the regions of strongest flow within the Agulhas Current. The amplitude and width estimated through the Gaussian fit method are therefore representative of the AC's dynamical core rather than of the total extent of south-westward flow associated with the AC. As seen in Figure 2a, the Gaussian fit method is able to successfully identify the position of the AC's dynamical core. The along-track altimetry shows that on average the AC core lies 113 km away from the coast, with the landward and seaward edges of the current core respectively 81 km and 145 km from the shore. The SST data shows an AC core generally positioned 124 km from the shore, with its landward and seaward edges located on average 85 km and 165 km from the shore. The mean width of the AC core derived from the SST is equal to 80 km, slightly in excess to that estimated from the along-track altimetry which averages to 64 km. Standard deviations in the AC's path varied

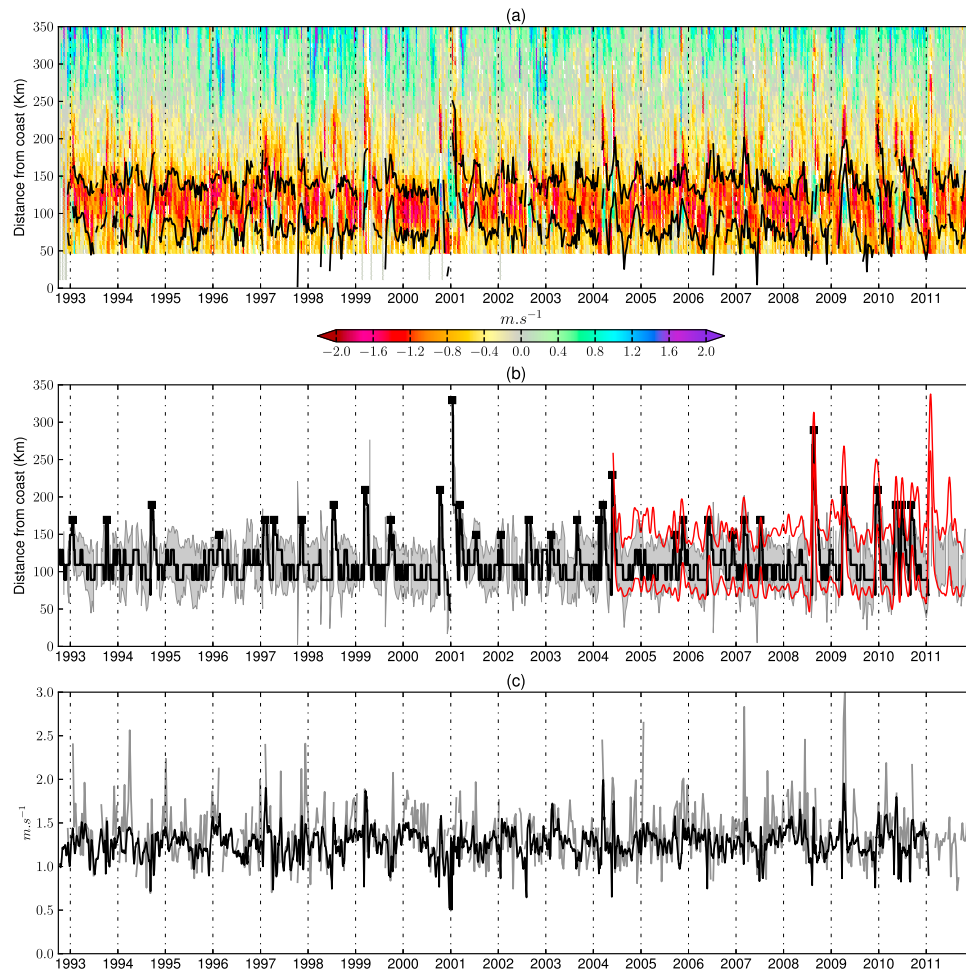


**Figure 2.** (a) Variations in across-track geostrophic current speeds along Track #020, from the coast to 350 km offshore. Black contour lines show the southern and northern walls of the AC core estimated through the Gaussian fit method. (b) Distance from the AC to the coast estimated from the merged altimetry, along-track altimetry and SST. Shades of grey show the width of the AC core estimated from along-track altimetry. Red lines indicate the edges of the AC core derived from the SST, while the black line shows the position of the AC core estimated from the AVISO merged-altimetry product. Black squares show variations in the AVISO-derived AC position exceeding 1 standard deviation from the mean. A 10-day Butterworth low-pass filter was applied to the SST data to remove outliers. (c) Amplitude of the Gaussian fit to the along-track altimetry (in grey) and absolute geostrophic current velocity at the AC core from the merged altimetry (in black).

between 25 km (SLA) and 30 km (SST). Fluctuations in the position of the AC core estimated from the along-track, merged altimetry and the SST are in very good agreement (Figure 2b). The central position of the AC core derived from the merged altimetry is strongly correlated to that estimated from the 1 Hz along-track altimetry with a Pearson correlation coefficient of 0.7 significant at the 95% confidence interval. The position of the AC core derived from the  $1/3^\circ$  gridded altimetry and the SST dataset (not shown) were also strongly correlated, with a correlation coefficient of 0.73 significant at the 95% confidence interval. In agreement with Rouault and Penven [2011], variations in the position of the AC are dominated by irregular offshore displacements associated with the southward propagation of meanders at the inshore border of the AC. Excursions in the path of the AC core exceeding 1 standard deviation from the mean are referred to as Pulses. These Pulses, plotted as black squares in Figure 2b occur on average 1.8 times a year and induce perturbations in the path of the AC which last for about 36 days. The two largest excursions in the path of the AC are

observed in January–February 2001 and August–September 2008, at times of anomalous upstream retroflexion of the AC (also referred to as Early Retroflexions). The largest of these excursions around the 12th of January 2001 occurs during the Early Retroflexion of 2000 [Rouault and Lutjeharms, 2003]. The second largest offshore perturbation in the AC occurred in mid-August 2008 and was a precursor to the Early Retroflexion event of 2008 [Rouault et al., 2010]. Data points coincident with the Early Retroflexion of 2000 have been flagged as the AC around that time could not be detected along Track #020. All other detected Pulses are associated with southward propagating meanders at the inshore edge of the AC. There appears to be more Pulses occurring beyond year 2001, with the annual number of Pulses increasing from about 1.3 to 2.2. Changes in the path of the AC do not display an annual cycle. Results from the analyses on the SST and along-track altimetry are not able to highlight annual variations in the width of the AC core.

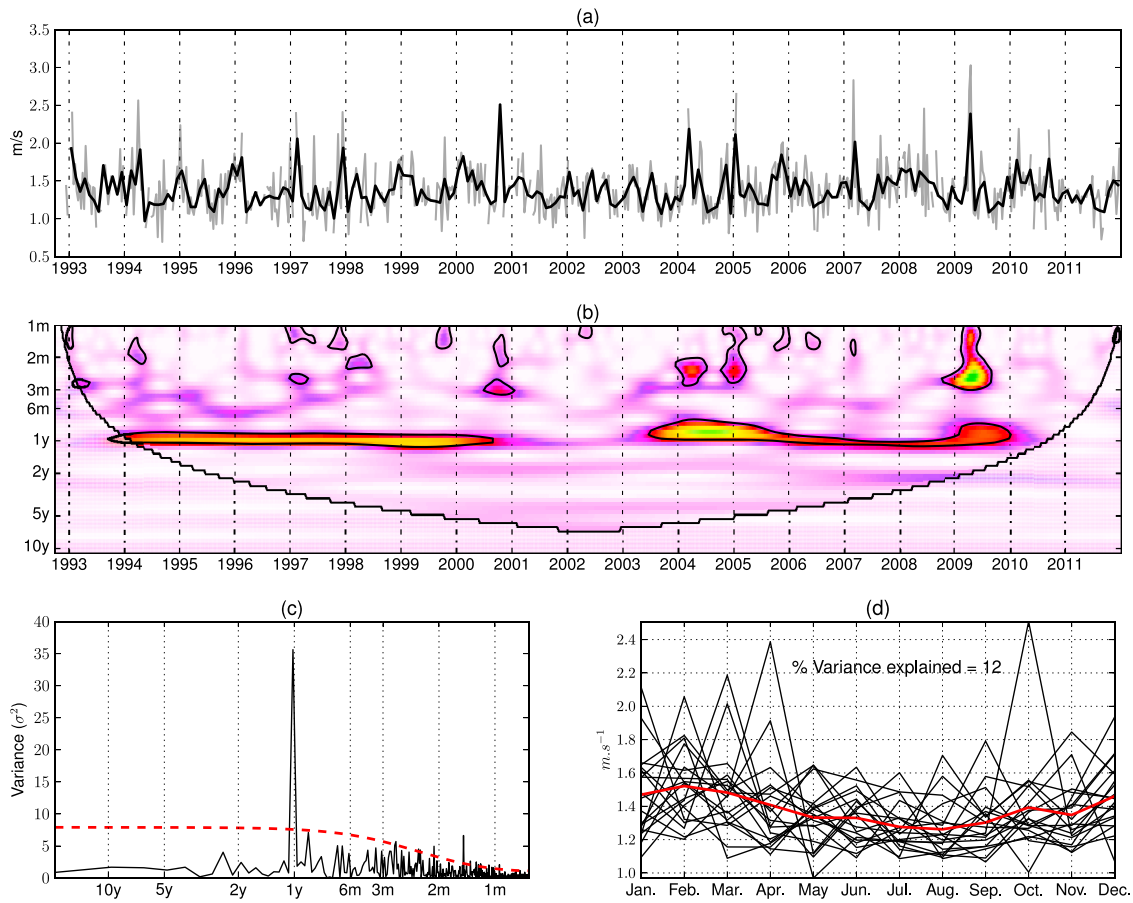


**Figure 3.** (a) Amplitude of the Gaussian fit to the AC core velocities derived from the 10-day along-track altimetry (in grey). Overlaid in black are the corresponding monthly averages. (b) Continuous wavelet transform of the Gaussian fit amplitudes, with black contour lines indicating the 95% confidence interval. (c) Power frequency spectra for the Gaussian fit amplitudes, the dashed red lines indicates the 95% confidence level. (d) Monthly seasonal variations of the Gaussian amplitudes with the climatology plotted as a thick red line.

[6] While the along-track altimetry, SST and merged altimetry are all able to successfully identify large fluctuations in the AC's path along Track #020, the AVISO gridded dataset is compromised by the spatial and temporal interpolation required to merge data from multiple altimeters and is not able to capture rapid or small scales fluctuations in the AC path (Figure 2b). Figure 2c also shows that current speeds at the AC core are strongly smoothed in the AVISO merged product; while AC core velocities estimated from the Gaussian fit method are associated with a standard deviation of  $0.32 \text{ m s}^{-1}$ , the standard deviation for the gridded AVISO current speed at the central position of the AC core only equals  $0.16 \text{ m s}^{-1}$ . The along-track altimetry dataset which has a higher resolution and has not been subject to spatial and temporal interpolation is able to successfully highlight rapid fluctuations in the AC over a wider range of scales. For this reason, in the following sections we use the output of the Gaussian fit analysis on the along-track altimetry to study the variability of the AC core.

#### 4. Variability in the Agulhas Current Stream

[7] Variations in Gaussian fit amplitudes (representative of the AC core flow strength) are plotted in Figure 3a. By following the AC it becomes possible to separate the

variability associated with offshore Pulses to that of the AC stream. This stream-coordinate approach reveals that although intra-annual frequencies associated with Pulses do modulate the strength of the flow within the dynamical core of the AC, the main spectral peak occurs at a period of 1 year. Both the wavelet (Figure 3b) and spectral analyses (Figure 3c) show that geostrophic current speeds in the AC core exhibit a strong annual cycle. Separate spectral analyses using both the AVISO gridded and along-track altimetry along the Jason-1 Track #198 located further south (not shown) confirm the dominance of the annual cycle on the variability of the geostrophic current speeds within the AC core. Seasonal variations in the geostrophic current speeds of the AC core show a stronger flow during the austral summer and weaker velocities experienced over the austral winter (Figure 3d). Seasonal geostrophic current speeds varied from  $1.5 \text{ m s}^{-1}$  in March to  $1.3 \text{ m s}^{-1}$  in July. In a high resolution (8 km) model of the southern AC, *Chang* [2009] finds seasonal variations in the AC maximum current speed near Track#020s of the same order of magnitude ( $0.1$  to  $0.2 \text{ m s}^{-1}$ ). At time-scales of a month or more, seasonal variations in the along-track geostrophic velocities within the dynamical core of the AC account for 12% of the signal's variance. In the monthly time-series of the AC core velocities

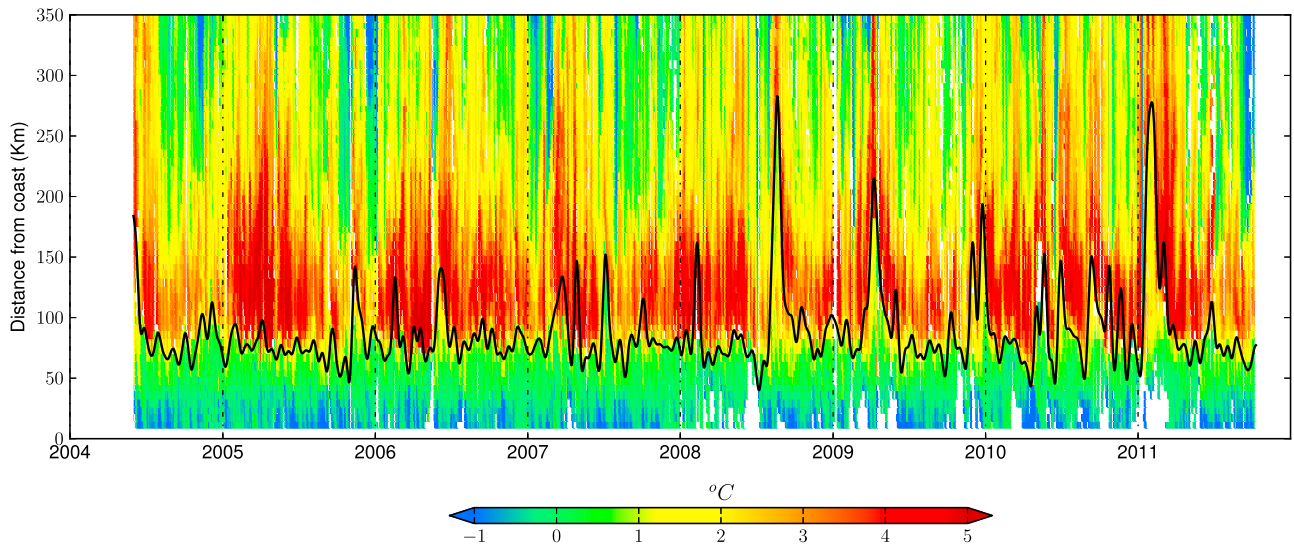


**Figure 4.** SST anomaly along Track #020. The black line shows the landward edge of the AC core derived from the SST imagery after applying a 10-day low-pass Butterworth filter. The SST anomaly is defined as the difference between the SST along Track #020 and the mean SST within 50 km off the coast.

extracted from the gridded AVISO dataset (not shown), the seasonal cycle accounts for 30% of the observed variance.

[8] Altimeters rely on the geostrophic approximation to derive ocean currents from horizontal gradients in SSH. But the SSH routinely measured by altimeters can be modulated by changes in the ocean circulation as well as steric heating due to the expansion or contraction of the water column [Kelly *et al.*, 1999]. Thermal variation in SSH can be expressed by

$$\eta_{steric} = \int_{-h_m}^0 \alpha_T T'_m dz \quad (1)$$

where  $T'_m$  is the temperature anomaly,  $h_m$  is the depth to which the temperature anomaly penetrates and  $\alpha_T$  is the coefficient of thermal expansion [Kelly *et al.*, 1999]. To verify that the seasonal variations observed in the geostrophic current velocities of the AC core are not induced by the seasonal cycle of SST and thus by steric effect, we use the observed SST along Track #020. Here, the temperature anomaly along the transect is defined as the difference between the SST along Track #020 and the mean SST within the first 50 km off the shore. In a color contour of the resulting temperature anomaly, the AC shows as a strong positive anomaly (Figure 4). Although SSTs in the AC and its coastal regions show strong seasonal fluctuations (not shown), the integrated SST gradient across the current's width does not exhibit a distinct annual cycle between June 2004 and October 2011. Our results suggest that annual variations in the absolute geostrophic current velocity at the AC core are not induced by steric heating.

[9] In their analyses of numerical ocean model outputs Biastoch *et al.* [1999] and Matano *et al.* [2002] argue that atmospheric forcing in the tropical regions of the western South Indian ocean modulates the strength of the AC transport through two of its source regions: the Mozambique channel and the East Madagascar Current. The link between wind forcing in the tropical south Indian ocean and annual variations in the Mozambique channel flow was confirmed

in a later study based on satellite observations and in-situ measurements [Ridderinkhof *et al.*, 2010]. Matano *et al.* [2008] however could not corroborate the connection previously established in numerical model outputs between the Mozambique flow and the AC transport at seasonal time-scales. Previous in-situ measurements have also not been able to highlight evidence of a seasonal cycle in the AC [Lutjeharms, 2006]. The inability of past observational studies to show a seasonality in the AC flow might be attributed to different dynamics at the measurement sites, the limited duration of the dataset analysed, or the Eulerian approach used for the analysis of the data. Our observations of an annual cycle in the AC core geostrophic flow are in agreement with results from numerical ocean models and seem to confirm the link between the wind-driven variability in the source regions of the AC and its transport further downstream. Our study also strongly emphasize the need for a stream-coordinate approach to adequately capture the variability of the AC.

## 5. Conclusion

[10] The region off Port Elizabeth is well suited to monitoring the variability of the AC. The position of the AC near Port Elizabeth does not display annual oscillations. Large perturbations in the AC path are caused by the southward passage of offshore meanders at the inshore edge of the AC. The size and duration of these meanders make them easily detectable using either altimetry or SST. Analysis conducted on the along-track altimetry and SST imagery could not reveal annual variations in the width of the AC's dynamical core. But the spectral analysis conducted on the AC core geostrophic current velocities revealed a distinct peak at the 1-year period. The annual cycle was the dominant mode of variability for absolute geostrophic currents within the AC's dynamical core. Considering the lack of seasonal variations in the width of the AC's dynamical core and the barotropic nature of the AC, it would be tempting to directly relate the annual changes observed in the AC geostrophic current

speeds to the overall AC volume transport. But further in-situ observations will be necessary to confirm whether absolute geostrophic currents within the AC core can be used as a proxy for the AC transport.

[11] **Acknowledgments.** Funding from the CSIR Ecosystem Earth Observation unit (PG EcoEO).

[12] The Editor thanks two anonymous reviewers for assisting in the evaluation of this paper.

## References

- Beal, L. M., W. P. M. de Ruijter, A. Biastoch, and R. Zahn (2011), On the role of the Agulhas system in ocean circulation and climate, *Nature*, 472 (7344), 429–436, doi:10.1038/nature09983.
- Biastoch, A., C. J. C. Reason, J. R. E. Lutjeharms, and O. Boebel (1999), The importance of flow in the Mozambique Channel to seasonality in the Greater Agulhas Current System, *Geophys. Res. Lett.*, 26(21), 3321–3324, doi:10.1029/1999GL002349.
- Bryden, H. L., L. M. Beal, and L. M. Duncan (2005), Structure and transport of the Agulhas Current and its temporal variability, *J. Oceanogr.*, 61, 479–492.
- Casal, T. G. D., L. M. Beal, R. Lumpkin, and W. E. Johns (2009), Structure and downstream evolution of the Agulhas Current system during a quasi-synoptic survey in February–March 2003, *J. Geophys. Res.*, 114, C03001, doi:10.1029/2008JC004954.
- Chang, N. (2009), Numerical ocean model study of the Agulhas Bank and the Cool Ridge, PhD thesis, Univ. of Cape Town, Cape Town, South Africa.
- Gilman, D. L., F. J. Fuglister, and J. M. Mitchell (1963), On the power spectrum of “red noise,” *J. Atmos. Sci.*, 20(2), 182–184.
- Gründlingh, M. L. (1983), On the course of the Agulhas Current, *S. Afr. Geogr. J.*, 65(1), 49–57.
- Kelly, K. A., S. Singh, and R. X. Huang (1999), Seasonal variations of sea surface height in the Gulf Stream region, *J. Phys. Oceanogr.*, 29(3), 313–327.
- Lee, J.-S. (1981), Refined filtering of image noise using local statistics, *Comput. Graphics Image Process.*, 15(4), 380–389, doi:10.1016/S0146-664X(81)80018-4.
- Lutjeharms, J. R. E. (2006), *The Agulhas Current*, Springer, Berlin.
- Matano, R. P., E. J. Beier, P. T. Strub, and R. Tokmakian (2002), Large-scale forcing of the Agulhas variability: The seasonal cycle, *J. Phys. Oceanogr.*, 32(4), 1228–1241.
- Matano, R. P., E. J. Beier, and P. T. Strub (2008), The seasonal variability of the circulation in the South Indian Ocean: Model and observations, *J. Mar. Syst.*, 74(1–2), 315–328.
- Meinen, C. S., and D. R. Watts (2000), Vertical structure and transport on a transect across the North Atlantic Current near 42°N: Time series and mean, *J. Geophys. Res.*, 105(C9), 21,869–21,891.
- Ridderinkhof, H., P. M. van der Werf, J. E. Ullgren, H. M. van Aken, P. J. van Leeuwen, and W. P. M. de Ruijter (2010), Seasonal and interannual variability in the Mozambique Channel from moored current observations, *J. Geophys. Res.*, 115, C06010, doi:10.1029/2009JC005619.
- Rio, M. H., S. Guinehut, and G. Larnicol (2011), New CNES-CLS09 global mean dynamic topography computed from the combination of GRACE data, altimetry, and in situ measurements, *J. Geophys. Res.*, 116, C07018, doi:10.1029/2010JC006505.
- Rouault, M., and J. R. E. Lutjeharms (2003), Microwave satellite remote sensing of sea surface temperature around southern Africa, *S. Afr. J. Sci.*, 99, 489–494.
- Rouault, M. J., and P. Penven (2011), New perspectives on Natal Pulses from satellite observations, *J. Geophys. Res.*, 116, C07013, doi:10.1029/2010JC006866.
- Rouault, M. J., A. Mouche, F. Collard, J. A. Johannessen, and B. Chapron (2010), Mapping the Agulhas Current from space: An assessment of ASAR surface current velocities, *J. Geophys. Res.*, 115, C10026, doi:10.1029/2009JC006050.
- van Sebille, E., L. M. Beal, and A. Biastoch (2010), Sea surface slope as a proxy for Agulhas Current strength, *Geophys. Res. Lett.*, 37, L09610, doi:10.1029/2010GL042847.